

# n- Gauge<sup>ST</sup> Case Study: Beam Profile Reflectometry Measurement of Cardiac Balloon Walls

## Abstract

Ten cardiac balloons were evaluated by *n*-Gauge<sup>ST</sup> to measure the thickness of the balloon walls using Beam Profile Reflectometry (BPR), a proprietary technique that collects data from a focused laser spot of typically <1 $\mu$ m diameter so that each measurement represents the result at a discrete location.

Measuring thickness on the *n*-Gauge<sup>ST</sup> is very straightforward, quick and simple to do. Typical balloon wall thicknesses observed were  $\sim$ 20 $\mu$ m, which were very close to what had been expected based on information provided beforehand by the manufacturer. Given the accuracy of the system and known calibration standard there is a high level of confidence in the results obtained.

## Introduction

Nightingale-EOS was approached to use its *n*-Gauge<sup>ST</sup> metrology device to characterise the wall thickness of a representative set of cardiac balloons. We were not asked to measure the balloons' external dimensions, tubing, or 'cone area' that joins the tube to the balloon; however, *n*-Gauge<sup>ST</sup> is easily capable of making these measurements, in conjunction with wall thickness, if required and configured to do so. All measurements were undertaken on deflated balloons as directed by the manufacturer.

## Principle of Beam Profile Reflectometry

Beam Profile Reflectometry (BPR) is a technique first used for measuring thin films on silicon wafers. Prior to the introduction of BPR, measuring reflectance as a function of angle involved complex and expensive hardware arrangements where both the light source and detector needed to be moved each time a new angle was selected.

As Figure 1 illustrates, BPR overcomes this limitation by using a high-magnification lens to bring a collimated laser beam to a sharp focus. At the focal point, which is typically less than 1 $\mu$ m across, light falls on the sample with the whole range of different angles-of-incidence through which the lens bends the light in order to achieve focus. After reflection, the lens recollimates the reflected light and there is a one-to-one correspondence between the physical location of a ray of light within the recollimated beam and the angle at which that ray was reflected from the surface. It is therefore possible to measure reflectance as a function of angle of incidence for a wide range of angles (typically, for a  $\sim$ 100X lens, a range of 0-60 degrees) simultaneously, with a very short data acquisition time, using an apparatus with no moving parts.

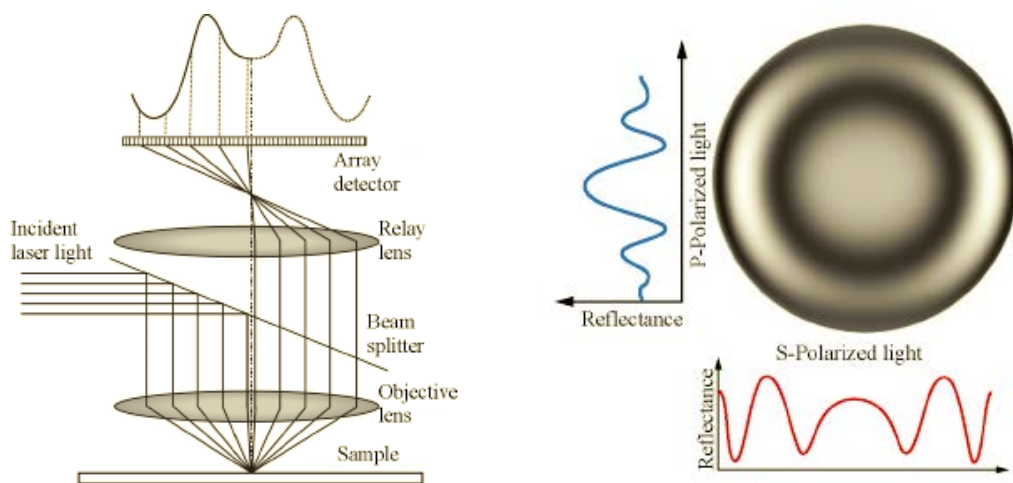


**Figure 1:** Schematic representation of a Beam Profile Reflectometry (BPR) system

When the beam profile is viewed after reflection from a coated surface or membrane, a characteristic 'bull's eye' pattern is seen due to the pattern of light and dark fringes that form as a result of the interference between rays reflected from the top of the film and those which penetrated to the bottom before being reflected. The amplitude of the fringes depends only on the refractive indices of the materials in the film. The period of the fringes is determined by the film thickness. It is therefore possible to decouple the effects of thickness and refractive index and measure the two classes of parameter independently.

While the 'bull's eye' pattern is symmetrical, as shown above, in the case of a flat level surface, if the surface is tilted or curved then a bull's eye pattern is still obtained but the centre moves around according to the orientation of the sample surface at the point where the beam is focused. Figure 2 shows an example of this. By locating the fringe centre automatically and taking proper account of the effect of sample tilt upon the fringe patterns, it is possible to obtain accurate measurements even from surfaces which are significantly tilted (typically, up to  $\pm 20^\circ$ ) and to measure the surface orientation as well as the thickness and index.

This greatly simplifies the taking of measurements from devices with complex or unpredictable shapes, since so long as the laser spot can be focused upon the sample surface there is no need to ensure that the surface is horizontal. In this specific case it was straightforward to measure balloons in their deflated state, where the surface orientation changed drastically as the laser spot moved from one end of the balloon to the other.

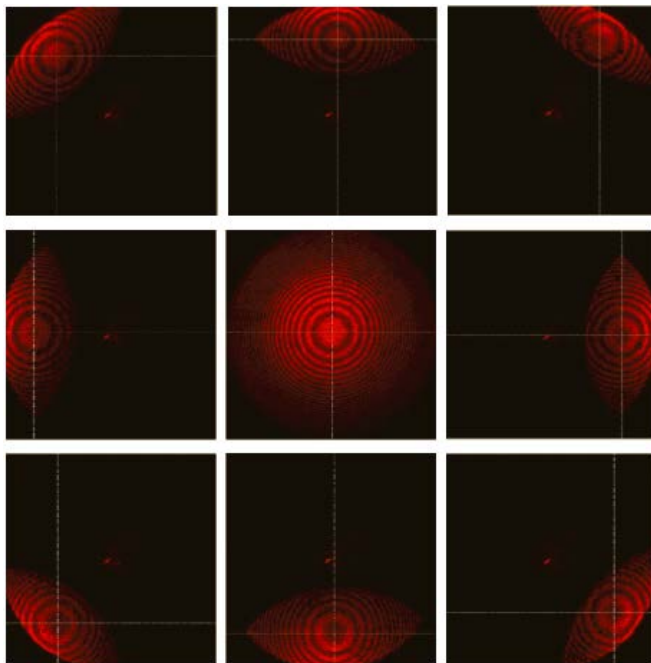


**Figure 2**

Illustration of how the BPR concentric fringe pattern changes with sample tilt. In this example, a set of measurements were taken from a contact lens which is horizontal in the middle and slopes away as the laser spot moves towards the edge. In each case, the thickness measurement can still be made and the centre locations provide additional information about the shape of the sample.

Compared to other measurement techniques, BPR's principal advantages are:

- There is no need for prior knowledge about the material's refractive index ( $n$ ), since this can be measured simultaneously with the thickness.
- There is no need for the orientation of the sample surface to be known at the time when the measurement is made: good results are obtained even if the sample surface is tilted by  $\pm 20^\circ$  when data is acquired.
- There is no need to scan the laser beam through the sample from one surface to the other, relying on the accuracy of a mechanical stage to obtain the measurement: the technique is entirely static and relies on no moving parts either in the optics or the sample-handling, save for what is required to locate the beam on the right part of the sample.

### Calibration

The  $n$ -Gauge<sup>ST</sup> system was calibrated with reference to a set of fused silica (pure SiO<sub>2</sub>) discs with thicknesses ranging from  $\sim 20\mu\text{m}$  to  $\sim 200\mu\text{m}$ . A 'master set' of discs has been measured on the company's behalf by the UK's National Physical Laboratory; these have been used to calibrate a reference  $n$ -Gauge<sup>ST</sup> in our laboratory, and the reference tool is then used to certify secondary 'transfer' standards

which can be supplied to customers alongside an *n*-Gauge<sup>ST</sup> system. The system used for this demonstration had been calibrated with reference to transfer set certified on the reference tool. We therefore have a high level of confidence that the calibration of the tool was accurate to within 1µm on all except possibly the ~50µm wafer, where the accuracy is within 2.5µm.

### Sample handling

All samples were placed on a flat microscope stage and light focused upon them. Collecting data from the balloons was straightforward and a case of simply focusing the laser beam onto the sample's surface. The samples did not appear to have any distinguishing marks, so were assumed to be equivalent to one another. Sample numbering in the next section therefore refers purely to the order in which the samples were removed from the packaging.

### Results

Measurements were made with no prior assumptions at all, measuring the thickness, refractive index, birefringence (related to stress in polymer films) and surface orientation at each point. The refractive index at the laser wavelength (640nm) was found to be stable at ~1.530 across the majority of measurement points. W1 to W5 refers to the number of separate wall thickness measurements taken along each balloon, with data obtained on each of the samples as follows:

#### Sample 1

Location	W1	W2	W3	W4
Thickness (µm)	20.2	21.0	20.6	21.4

#### Sample 2

Location	W1	W2	W3	W4	W5
Thickness (µm)	19.2	18.9	19.7	17.6	17.6

#### Sample 3

Location	W1	W2	W3	W4	W5
Thickness (µm)	20.0	19.5	21.1	20.3	19.9

#### Sample 4

Location	W1	W2	W3	W4	W5
Thickness (µm)	20.7	19.2	17.9	17.8	18.8

#### Sample 5

Location	W1	W2	W3	W4	W5
Thickness (µm)	19.5	19.3	19.3	22.3	19.8

#### Sample 6

Location	W1	W2	W3	W4	W5
Thickness (µm)	20.2	19.2	19.7	19.3	19.3

#### Sample 7

Location	W1	W2	W3	W4	W5
Thickness (µm)	20.1	20.0	19.1	19.6	19.0

#### Sample 8

Location	W1	W2	W3	W4	W5
Thickness (µm)	19.8	20.4	20.0	20.7	20.7

#### Sample 9

Location	W1	W2	W3	W4	W5
Thickness (µm)	20.6	19.1	20.6	21.0	20.1

#### Sample 10

Location	W1	W2	W3	W4	W5
Thickness (µm)	19.9	20.4	20.6	21.0	21.1

## Discussion and Conclusion

The results from each sample show a very consistent balloon wall thickness of  $\sim 20\mu\text{m}$ . Along the balloons themselves, there was no particular relationship between thickness and position, except that there is usually less than a micron of variation along the length of the balloon and some balloons (e.g. sample 1) are consistently thicker than others (e.g. sample 2).

Typical data-acquisition time at each point was about one second and the analysis / calculation time was around three seconds on a laptop computer. If the sample were held in a suitably-designed jig to facilitate the precise positioning of the laser spot, and especially if the sample handling were to be motorised, then an expected cycle time of 20-30 seconds per sample is achievable.

Measuring the thicknesses of balloon walls on an *n*-Gauge<sup>ST</sup> is simple, reliable and repeatable and produces results very close to the value expected.

*Note: The data and conclusions in this case study are provided for information only not be used or interpreted for any other purpose.*

### Further Information:

Cliff Murphy  
Nightingale-EOS Limited  
Unit 2, Bryn Estyn Business Centre, Bryn Estyn Road,  
Wrexham, LL13 9TY, United Kingdom  
enquiries@n-eos.com - <http://www.n-eos.com>  
+44 (0) 7810 502830 • +44 (0) 1978 351711

